www.ugb.org.br
ISSN 2236-5664

Revista Brasileira de Geomorfologia

v. 21, nº 2 (2020)

http://dx.doi.org/10.20502/rbg.v21i2.1671

# MACHINE LEARNING ALGORITHM IN THE PREDICTION OF GEOMORPHIC INDICES FOR APPRAISAL THE INFLUENCE OF LANDSCAPE STRUCTURE ON FLUVIAL SYSTEMS, SOUTHEASTERN - BRAZIL

# ALGORITMO DE APRENDIZADO DE MÁQUINA NA PREDIÇÃO DE ÍNDICES GEOMÓRFICOS PARA AVALIAÇÃO DA INFLUÊNCIA DA ESTRUTURA DA PAISAGEM EM SISTEMAS FLUVIAIS, SUDESTE – BRASIL

***Cristiano Marcelo Pereira de Souza***
*Programa de Pós-Graduação em Geografia, Universidade Estadual de Montes Claros*
*Av. Dr. Ruy Braga, S/N, Montes Claros, Minas Gerais. CEP: 39401-089. Brasil*
*ORCID: 0000-0001-7692-1613*
*E-mail: cristiano.souza@ufv.br*

***Natália Aragão de Figueredo***
*Colégio Militar de Juiz de Fora*
*Av. Presidente Juscelino Kubitschek, 5200, Juiz de Fora, Minas Gerais. CEP: 36087-000. Brasil*
*ORCID: 0000-0003-3398-7107*
*E-mail: nataliaragao@gmail.com*

***Liovando Marciano da Costa***
*Programa de Pós-Graduação em Solos Nutrição de Plantas, Universidade Federal de Viçosa*
*Av. Peter Henry Rolfs, s/n, Viçosa, Minas Gerais. CEP: 36570-900. Brasil*
*ORCID: 0000-0001-9581-0783*
*E-mail: liovando@yahoo.com.br*

***Gustavo Vieira Veloso***
*Programa de Pós-Graduação em Solos Nutrição de Plantas, Universidade Federal de Viçosa*
*Av. Peter Henry Rolfs, s/n, Viçosa, Minas Gerais. CEP: 36570-900. Brasil*
*ORCID: 0000-0002-9451-2714*
*E-mail: gustavo.v.veloso@gmail.com*

***Maria Ivete Soares de Almeida***
*Programa de Pós-Graduação em Geografia, Universidade Estadual de Montes Claros*
*Av. Dr. Ruy Braga, S/N, Montes Claros, Minas Gerais. CEP: 39401-089. Brasil*
*ORCID: 0000-0002-3257-7109*
*E-mail: ivetegeo@yahoo.com.br*

***Expedito José Ferreira***
*Programa de Pós-Graduação em Geografia, Universidade Estadual de Montes Claros*
*Av. Dr. Ruy Braga, S/N, Montes Claros, Minas Gerais. CEP: 39401-089. Brasil*
*ORCID: 0000-0001-8125-6806*
*E-mail: expedito.jferreira@gmail.com*

**Informações sobre o Artigo**

Recebido (Received):
19/06/2019
Aceito (Accepted):
12/03/2020

**Keywords:**
Hydrographic Basin; Structural Drainage Control; Random Forest; Morphotectonic Analysis;

**Palavras-chave:**
Bacia Hidrográfica; Controle Estrutural da Drenagem; Random Forest; Análise Morfotectônica;

**Abstract:**

The Abaeté hydrographic basin was influenced by sediments (Proterozoic and Cretaceous) and by volcanism (Upper Cretaceous). The objective was to identify whether the drainage configuration is due to structural factors or by neotectonics. We use geomorphic indices (Basin Asymmetry Factor, Stream Length-gradient Index - SL, and Channel Steepness Index - $k_{sn}$). We elaborate longitudinal profiles in the rivers of sub-basins. We apply the Random Forest (RF) Machine Learning algorithm in the prediction of the SL and $k_{sn}$ indices, with the selection of relevant covariates. The RF was efficient in predicting, with better performance in the $k_{sn}$ ($R^2$ 0.38), and indicating the areas of influence of the indices. The highest values of the indices are in zones of lithological contact with different resistances, favoring a sharp change in channel slope (knickpoints). In these zones, there is also a predominance of sub-basins tilted, and the longitudinal profiles of the rivers show uplift or subsidence. Therefore, structural factors conditioned the drainage of the basin.

**Resumo:**

A bacia hidrográfica de Abaeté foi influenciada por sedimentação (Proterozóico e Cretáceo) e processo vulcânicos (cretáceo superior). O objetivo foi identificar se há um controle estrutural dos sistemas fluviais relacionado ao vulcanismo ou por neotectônica. Utilizamos os índices geomórficos (Fator de Assimetria de Bacia, Stream Length-gradient Index – SL, e Channel Steepness Index - $k_{sn}$); elaboramos perfis longitudinais nos rios de sub-bacias. Aplicamos o algoritmo de Aprendizado de Máquina Random Forest (RF) na predição dos índices SL e $k_{sn}$, com seleção de covariáveis importantes. O RF foi eficiente na predição, com melhor performance em $k_{sn}$ ($R^2$ 0,38), e indicando as áreas de influência dos índices. Os valores mais altos dos índices estão em zonas de contato litológico com diferentes resistências, favorecendo mudanças acentuadas de declividade no canal (knickpoints). Nessas zonas, também há predominância de sub-bacias basculhadas, e os perfis longitudinal dos rios mostram elevação ou subsidência. Portanto, fatores estruturais condicionam os sistemas fluviais da bacia.

## 1. Introduction

The river systems are sensitive to the evolution of the relief, generating changes in the morphology of the rivers (FONT *et al.*, 2010), abrupt changes in slope in the longitudinal profile of the river (AMBILI & NARAYANA, 2014), and asymmetric basins (EL HAMDOUNI *et al.*, 2008). Therefore, studies use analysis of the drainage network to identify structural control (KALE *et al.*, 2014), and also deformations by neotectonics (GARROTE *et al.*, 2008; MONTEIRO *et al.*, 2010; ALVES *et al.*, 2019).

Visual assessment of drainage characteristics is essential, but quantitative methods are complementary and make the analysis more objective, and geomorphic indices perform this function. Among these indices, the Stream Length-gradient Index method (SL), identifies abrupt changes in slope along the profile (knickpoints) (HACK, 1973). Based on the SL indices, the Normalized channel steepness index ($k_{sn}$) (WOBUS *et al.*, 2006), has the advantage of inserting variables according to the drainage characteristics (CASTILLO *et al.*, 2014). There is also the Basin Asymmetry Factor index, capable of identifying tilted hydrographic basin (HARE & GARDNER, 1985). Studies demonstrate the efficiency of these methods in different geological contexts (GARROTE *et al.*, 2008; FONT *et al.*, 2010; MONTEIRO *et al.*, 2010; CYR *et al.*, 2014; SOUZA & PEREZ FILHO, 2017), providing a quick assessment for large areas, and with quantitative data.

The geographic information system (GIS) combined with topographic data from digital elevation models (DEM), represent an advance in the extraction of geomorphic indices (TROIANI *et al.*, 2014; ALVES *et al.*, 2019). However, some data may have limitations in cartographic representation, for example, the SL and $k_{sn}$ indices are represented by points (MONTEIRO *et al.*, 2010) or by drainage network (EL HAMDOUNI *et al.*, 2008; CASTILLO *et al.*, 2014). Therefore, to advance the cartographic representation, studies use kriging methods, creating homogeneous zones of influence of the indices (knickzones) (PÉREZ-PEÑA *et al.*, 2009; FONT *et al.*, 2010). However, kriging efficiency depends on point density, spatial dependence and anisotropy (OLIVER & WEBSTER, 1990); therefore, these characteristics that can be limiting, justify testing new methods of prediction.

Recently, Machine Learning algorithms (ML) has gained prominence in spatial prediction studies. In general, ML has the advantage of performing spatialization from point values (variable), based on a database in raster format (predictive covariates), and using some statistical algorithm (KUHN & JOHNSON, 2013). Studies show the efficiency of ML in the area of geology (CRACKNELL *et al.*, 2014), geomorphology (MOHAMMADY *et al.*, 2019) and pedology (SOUZA *et al.*, 2018; GOMES *et al.*, 2019). Besides, ML can perform better than the kriging method (CLODOALVES, 2019), especially when the variables do not have spatial dependence; however, there are no studies on the prediction of geomorphic indices with ML.

Most studies with geomorphic indices are on tectonically active margins, focusing on neotectonics (SEEBER & GORNITZ, 1983; TROIANI *et al.*, 2014). However, in Brazil, passive margin, some studies attest to the occurrence of neotectonic processes, by abrupt changes in river direction, knickpoints, and straight rivers (ETCHEBEHERE *et al.*, 2004; SOUZA *et al.*, 2011; DORANTI-TIRITAN *et al.*, 2014), with some characteristics quantified by geomorphic indices.

In Brazil, major tectonic events occurred mainly in the separation of the South American continent with Africa, with successive continental lava spills, becoming the largest in the world, since the late Jurassic (FODOR & HANAN, 2000). However, post-rift-phase, the South American plate passed over a thermal anomaly (Trindade hotspot), promoting intense magmatism (alkaline and basaltic) (FRAGOSO *et al.*, 2011). The phenomenon formed kamafugite volcanic and subvolcanic rocks, recognized, in addition to Brazil, in two locations in the world, in Africa (Uganda and Zaire) and Europe (northeast of Italy) (SGARBI, 2000).

In addition to the deposition of volcanic materials (Cretaceous), such events also generated a set of geological faults (SGARBI, 2000), with the possibility of reactivation in the Quaternary, being able to change the morphology of the current drainage. Some studies demonstrate reactivation processes in the interior of Brazil, for example, in the region of Poços de Caldas-Minas Gerais, by reactivation of the Triassic shear zones (GROHMANN *et al.*, 2007; DORANTI-TIRITAN *et al.*, 2014).

This study aims to identify evidence of structural and/or neotectonic control using geomorphic indices and prediction methods of indices by the Machine Learning. The study area is the Abaeté hydrographic basin, located in the central portion of the state of Minas Gerais, where there was an intense process of sedimentary deposition during the Proterozoic and volcanism in the Cretaceous.

### 1.1 Physiography and geological framework

The study area is the Abaeté hydrographic basin, located in southeastern Brazil (Minas Gerais state), between the coordinates -17 ° 85 'to -19 ° 36' latitude S -45 ° 21 'to -46 ° 31' longitude W, with an area of 5,824 km$^2$ (Figure 1). The climatic domain is Cwa (Köppen classification), with an average annual precipitation of 1,700 mm.

The basin has Proterozoic and Cretaceous sedimentary rocks and the influence of magmatic activity during the Cretaceous (Figure 1). In general, in Proterozoic lithologies, occur depressions and dissected areas. On the other hand, the Cretaceous rocks form plateaus, forming two morpho sculptural compartments, one preserved surface (Mata da Corda Group), the other dissected (Areado Group) (OLIVEIRA & RODRIGUES, 2007).

The first sedimentation occurred Proterozoic forming the Bambuí Group rocks, predominantly siliciclastic mixed with carbonate (UHLEIN *et al.*, 2019). The Lagoa Formosa Formation corresponds to older deposits, occurring upstream of the basin. The Formation is composed predominantly of Siltite, with small intercalations of Clay Siltite, Argilite, and in lesser quantity Sandstone. In general, the outcrops are intensely fractured and very weathered (FRAGOSO *et al.*, 2011).

The Serra de Santa Helena Formation occurs as a small strip downstream of the basin, limited by two faults SW-SE direction. They are predominantly pelitic sediments, with Slates, Siltstones, Shales and fine Quartzites, Limestones, dark Metapelites and Marble. The Serra da Saudade Formation (Neoproterozoic) has a larger area, with shales, green Argilites and Siltstones ("Verdete") (LIMA *et al.*, 2007). In this region, the drainage has high sinuosity indicating structural control, and there are some fault systems (SW-SE). The Três Marias Formation occurs in the downstream, with the presence of Arcosean Sandstones, Sandstones and Siltstones. The rocks are fractured, and the main river flows over a geological fault (FRAGOSO *et al.*, 2011).

The second sedimentation process occurred in the Cretaceous and is related to crustal stretching generated during the opening of the South Atlantic. This extensional phase produced a basin with a Graben/Horst system (FRAGOSO *et al.*, 2011). The region was filled with predominantly continental sediments (Grupo Areado), forming pinkish to reddish and yellow sandstones, with the presence of fractures. The rocks form mainly the basal part of the basin plateaus, where the drainage has sections with subsidence.

In Upper Cretaceous, volcanic processes occurred in the region, forming the Mata da Corda Group, and are currently at the top of the plateaus. These are alkaline rocks of effusive, pyroclastic, plutonic, and epiclastic origin, due to spills and even of explosive origin (Kamafugites) (FODOR & HANAN, 2000; BAGGIO *et al.*, 2015).

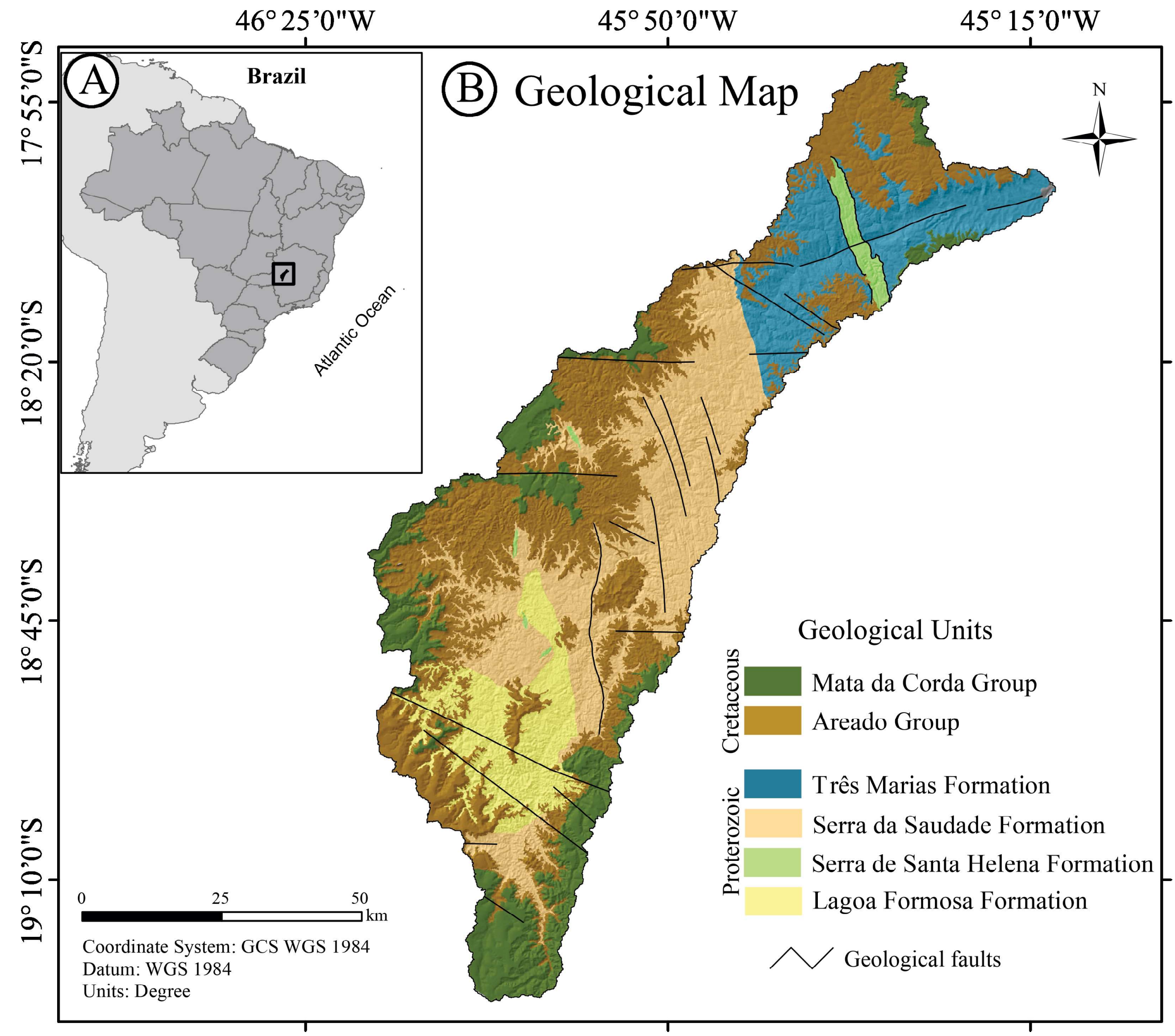


*Figure 1 - (A) location of the study area; and (B) Geological map of the Abaeté basin.*

## 2. Materials and Methods

### 2.1 Longitudinal profile and geomorphic indices

We used Digital Elevation Model (DEM) 1 arc-second Shuttle Radar Topographic Mission (SRTM) (JARVIS *et al.*, 2008) to extract the drainage network and delimit sub-basins based on the drainage order ≥ 4 (STRAHLER, 1957).

We elaborate longitudinal profiles for each sub-basin associating the DEM and the main river. The profiles allow identifying anomalous sections of the drainage in relation the best fit line with a coefficient $R^2 > 0.80$. We consider anomalous stretches (subsidence/uplift) the distances greater than 10 m, referring to the best fit line (SANTOS *et al.*, 2011).

We applied three geomorphic indices, Basin Asymmetry Factor (AF), Stream Length-gradient Index (SL), and Normalized Channel Steepness Index ($k_{sn}$). The AF indices allow the identification of tilted sub-basins (EL HAMDOUNI *et al.*, 2008). AF values close to or equal to 50 indicate that the basin is symmetrical. Values > 50 indicate tilting of the right bank of the river (facing downstream), and values < 50 indicate tilting of the left margin of the basin (Equation 1)

$$AF = (Ar/At).100 \qquad \text{Equation 1}$$

where AF: basin asymmetry factor; Ar: right basin area (i.e., facing downstream); and At: total area of the drainage basin.

The Stream Length-gradient Index (SL) allow assessing drainage anomalies (HACK, 1973). In general, the longitudinal profile of the river tends to exhibit concave curvature, while abrupt changes in slope are considered anomalous conditions and appear as steps along the river (knickpoints). The knickpoints may be related to differential erosion of rocks, lower flow tributary junction, and upstream erosion due to lower base level; once discarding these possibilities, neotectonics appears as an explanation (KELLER & PINTER, 1996). To calculate the SL index, we use the Knickpoint Finder software (QUEIROZ *et al.*, 2015). The software calculates the index for the total drainage extent (SLt), for segments (SLs), and determines classes of anomalies based on the SLs/SLt ratio (SEEBER & GORNITZ, 1983). (SLs/SLt > 10 1st order anomalies, between 2 and 10, 2nd order anomalies, and < 2 without anomalies). Equations 2, 3 and 4, respectively.

$$SLt=\frac{\Delta H}{\ln(L)} \qquad \text{Equation 2}$$

$$SLs =\left(\frac{\Delta h}{\Delta l}\right) L \qquad \text{Equation 3}$$

$$SLs/SLt = \frac{SLs}{SLt} \qquad \text{Equation 4}$$

where: L: total length of the channel; ΔH: elevation difference between the extremes of a given stream reach; Δh = elevation difference in the segment; Δl = length of the segment.

We used the Normalized Channel Steepness Index ($k_{sn}$) (WOBUS *et al.*, 2006), which is derived from the slope–area regression, and generates a normalization of the variables by the channel concavity indices (Equation 5).

$$S=K_s \times A^{-\theta} \qquad \text{Equation 5}$$

where S: channel slope; $K_s$: channel–steepness index; A: drainage area (surrogate of stream discharge); θ: concavity index (slope–area regression).

The $k_{sn}$ index allows correlating rates of uplift and denudation of a hydrographic basin concerning the evolution of longitudinal profiles. Regarding the concavity index ($\theta$ref), the value of 0.45 is generally used, which is a reference for bedrock rivers (CASTILLO *et al.*, 2014). However, the applicability of $\theta$ref in mixed alluvial-bedrock channel can lead to misinterpretations. Therefore, we chose to calculate a specific value of $\theta$ for each sub-basin (SOUZA & PEREZ FILHO, 2017), where $\theta$ is obtained from the linear regression values of the correlation between the slope and the accumulated area in log-log. The variables to obtain the $k_{sn}$ index were inserted in Topotoolbox 2.0 in programming language Matlab®, it is a set of scripts to extract $k_{sn}$ values from a DEM automatically (SCHWANGHART & SCHERLER, 2014).

### 2.2 Spatial prediction SL and $k_{sn}$ indices

We applied a methodological framework in R software (RCORE TEAM, 2016) to predict the SL and $k_{sn}$ indices (Figure 2). The script is with the Random Forest algorithm, which performs classification and regression analysis and allows data to be predicted for non-sampled areas (BREIMAN, 2001). The RF uses a group of covariates and provides statistics on the precision and uncertainty of the prediction process.

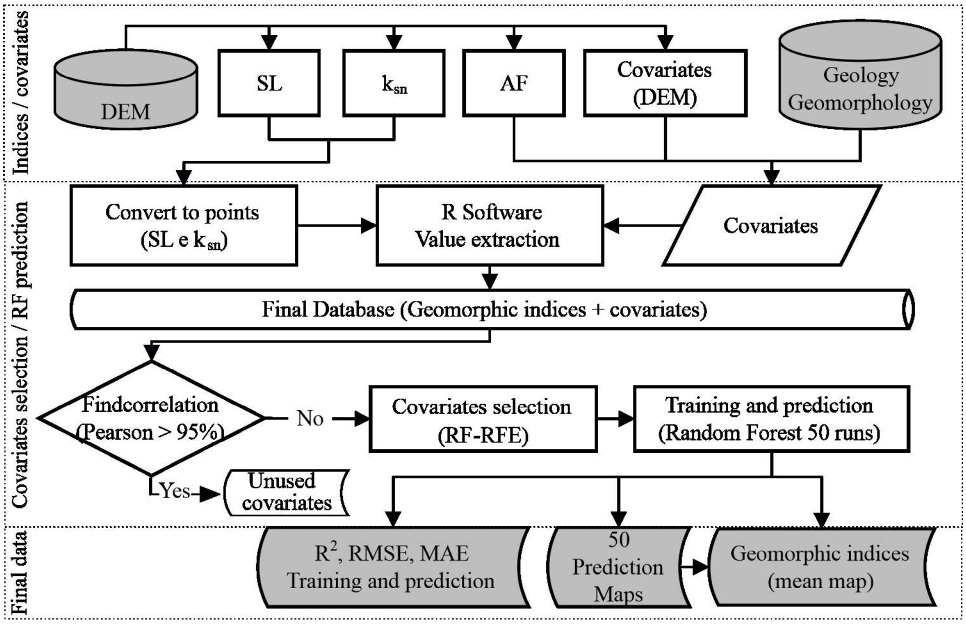


*Figure 2 - Flowchart of the methodological sequence to obtain the geomorphic indices (AF, SL e ksn), the predictive covariates, and the prediction process with Random Forest algorithm with selection of important covariates, and 50 times training and validation process.*

The RF uses point data (variable), but the $k_{sn}$ is represented by a drainage network. To associate this information, we convert the results from $k_{sn}$ to raster and extract the value at each point in SL. Another step, consisted in the elaboration of the covariate database (raster format). SRTM geomorphometric covariates (36), listed in Gomes *et al.* (2019); Sena *et al.* (2020); geology and geotectonic map (2) (PINTO *et al.*, 2003); geomorphology map (1); and asymmetry factor (1).

In general, spatial prediction studies using ML, indicate that the excess of covariates does not guarantee better results, and also increases the computational processing time (KUHN & JOHNSON, 2013; SOUZA *et al.*, 2018; GOMES *et al.*, 2019). To reverse this problem, we applied two steps: (i) we discard covariates with high correlation concerning the database (Pearson > 95%) by findcorrelation (KUHN & JOHNSON, 2013); (ii) we selected a group of covariates by RFE (Random Forest-Recursive Feature Elimination) (GRANITTO *et al.*, 2006; KUHN & JOHNSON, 2013), and the ideal subset criterion was an $R^2$ with a 3% decrease concerning the subset with the highest $R^2$.

The prediction uses the subset of covariates selected by RF-RFE. However, to avoid a biased prediction process, we generate the prediction 50 times. During each step, the RF algorithm randomly selects 75% of the samples for training and validates with 25%. This process is essential because it indicates the variability of the prediction since different clusters of data generate different results (KUHN & JOHNSON, 2013). The result is 50 maps for each geomorphic index, and the average of the maps is the final result.

The model also provides statistical data that shows accuracy (coefficient of determination $R^2$) and error (root mean squared error RMSE, and mean absolute error MAE), usual procedures in ML (KUHN & JOHNSON, 2013; CHAGAS *et al.*, 2018; SOUZA *et al.*, 2018; GOMES *et al.*, 2019). The values of $R^2$ RMSE and MAE are obtained with equations 6, 7 and 8, respectively.

$$R^2 = 1 - \frac{\sum_n (X_{obs,i} - X_{mod,i})^2}{\sum_n (X_{obs,i} - \bar{X})^2} \qquad \text{Equation 6}$$

$$RMSE = \sqrt{\frac{\sum_{i=1}^{n} (X_{obs,i} - X_{mod,i})^2}{n}} \qquad \text{Equation 7}$$

$$MAE = \frac{\sum_{i=1}^{n} \left| X_{obs,i} - X_{mod,i} \right|}{n} \qquad \text{Equation 8}$$

where $x_{obs}$ is the observed value; $x_{mod}$ is the predicted value by the use of the Machine Learning algorithm; $n$ is the number of observations.

The analysis of the geomorphic indices was supported by the comparative analysis with other information (geology, geomorphology, drainage configuration, longitudinal profile, geomorphometric data, and basin asymmetry).

## 3. Results

The sub-basins tend to be symmetrical in the areas of lower elevation with smoothed reliefs, and the sub--basins tilted are located to the south, in escarpment areas of the highlands, showing similar tilting direction (Figure 3). The region has geological faults, predominantly perpendicular to the rivers, except in the downstream area, where there is a fault in the main river bed.

The longitudinal profiles showed that in the zones of lithological contacts, there is an uplift or subsidence of the profile concerning the best fit line (Figure 4). For example, the uplift of the profile occurs in rocks of the Três Marias Formation (sub-basins 1 and 2), whereas, in the contact areas of the Mata da Corda/Areado Groups, there is a predominance of subsidence (sub-basins 4 e 5).

The SL indices identified 912 points (knickpoints), with maximum values of 50 SLt, 783 SLs, and 26 SLs/SLt. The $k_{sn}$ indices classified 1,715 km of drainage, with a maximum value of 293 and an average of 42.

The prediction of indices by ML used covariates to assist in the prediction (KUHN & JOHNSON, 2013; SOUZA *et al.*, 2018). From the findcorrelation and RF-RFE function, a maximum of 11 covariates was selected in the prediction in the SLt, and a minimum of 7 in the SLs/SLt, ranked by level of importance (Table 1). Among the covariates, three predominated in the selection of the RFE, (Ls Factor, Standardized Height, Morphometric Protection index), and the geology covariate was significant in the second $k_{sn}$ prediction level.

The prediction process was efficient; the values of $R^2$ in training and validation were similar, showing low overfitting (KUHN & JOHNSON, 2013). The highest $R^2$ was in $k_{sn}$ ($R^2$ 0.38) and lower in SLs/SLt (0.25). The RMSE and MAE evaluate the error in the prediction process, and the values are expressed in units of the analyzed variable (KUHN & JOHNSON, 2013). Therefore, in our results, the RMSE and MAE were below the average in each index, and there was low variation (CV% variation coefficient) in the 50-runs predictions. CV% was higher than 10% only in the SLs and $k_{sn}$ indexes, while the majority was <5 (Tables 1 and 2).

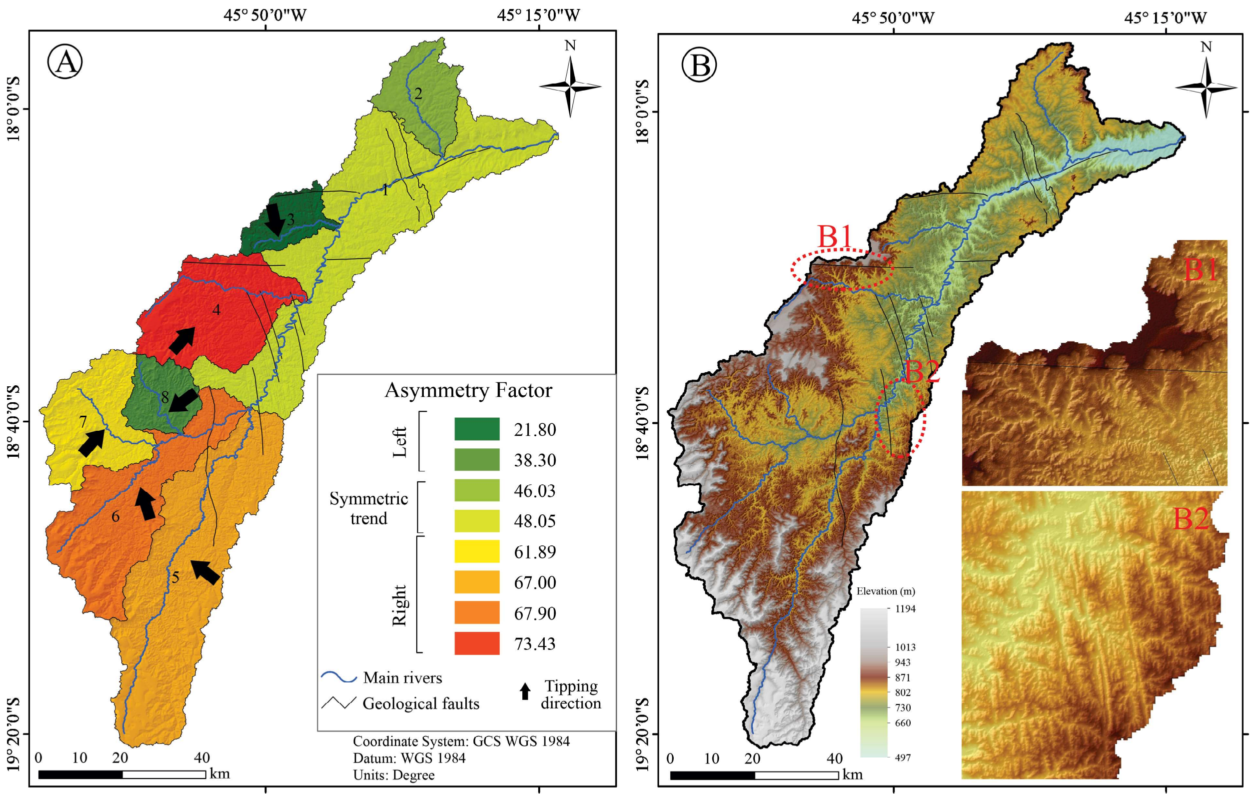


*Figure 3 - (A) Asymmetry factor of sub-basins (AF) and tipping direction; (B) Digital elevation model, indicating sinuous relief fronts associated with geological faults (B1), and rectilinear relief fronts (B2).*

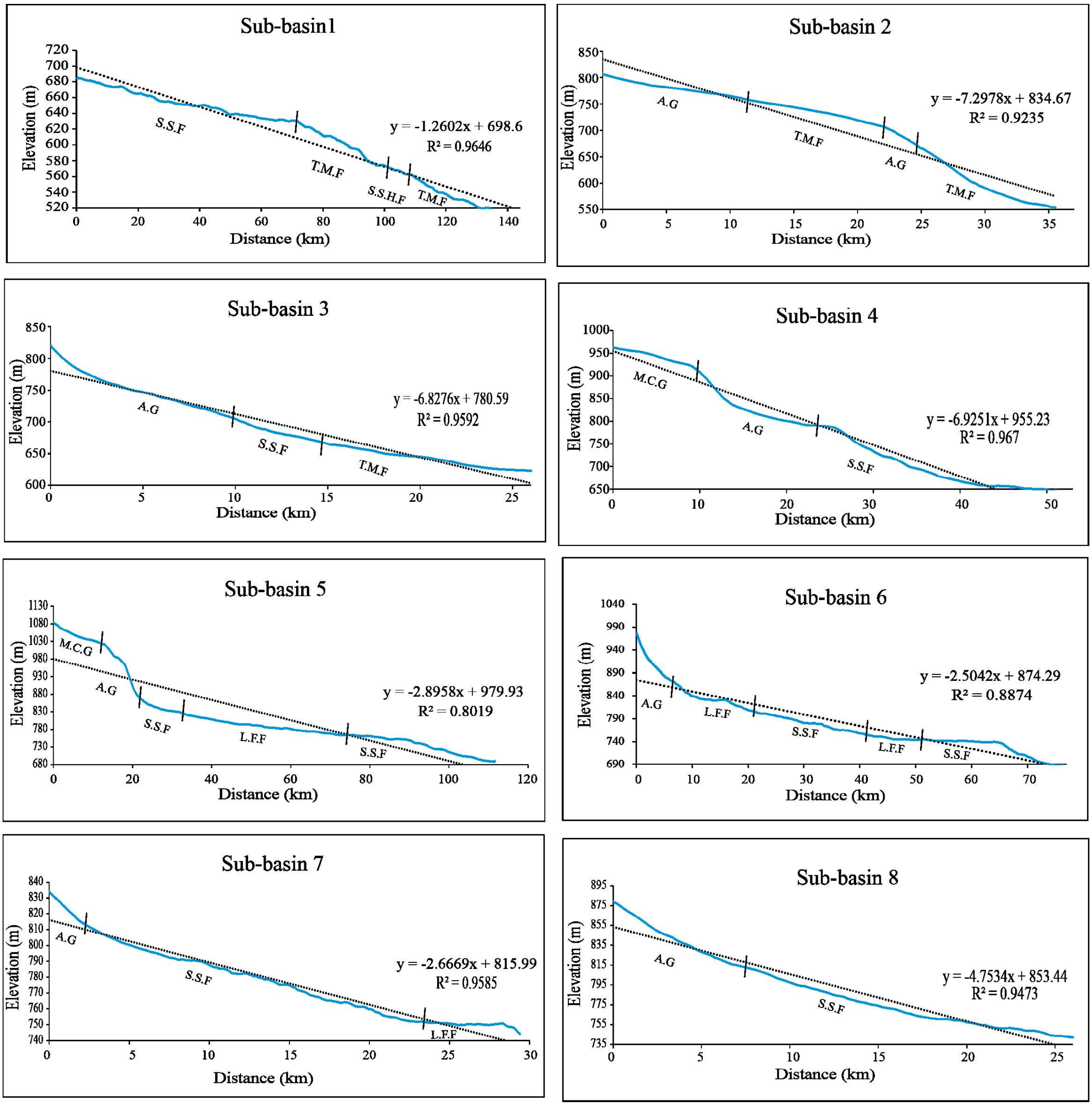


*Figure 4 - Longitudinal profiles of rivers in the sub-basins and identification of lithological changes (vertical lines). A.G: Areado Group; M.C.G: Mata da Corda Group; L.F.F: Lagoa Formosa Formation; T.M.F: Três Marias Formation; S.S F: Serra da Saudade Formation; S.S.H.F: Serra de Santa Helena Formation.*

**Table 1: Performance of the Random Forest algorithm and selection of covariates using RF-RFE in the prediction of geomorphic indices.**

| Variable | $R^2$ | RMSE | X1 | X2 | X3 | X4 | X5 | X6 | X7 | X8 | X9 | X10 | X11 |
|---|---|---|---|---|---|---|---|---|---|---|---|---|---|
| SLt | 0.25 | 9.22 | 2 | 1 | 5 | 7 | 11 | 12 | 9 | 14 | 3 | 16 | 15 |
| SLs | 0.27 | 104.52 | 1 | 3 | 2 | 8 | 10 | 13 | 15 | 15 | ns | ns | ns |
| SLs/SLt | 0.13 | 4.55 | 1 | 3 | 6 | 8 | 7 | 2 | 15 | ns | ns | ns | ns |
| $K_{sn}$ | 0.38 | 25.90 | 1 | 4 | 2 | 9 | 7 | 14 | 3 | 12 | 16 | ns | ns |

*X1, X2... X11: Importance levels; 1: LS factor; 2: Standardized Height; 3: Morphometric protection index; 4: Geologia; 5: Normalized height; 6: Curvature profile; 7: Cross Sectional Curvature; 8: Curvature longitudinal; 9: Channel base level; 10: Slope; 11: Mid slope positon; 12: DEM; 13: Real surface area; 14: Terrain surface texture; 15: Curvatute minimal; 16: Slope height; ns: Not selected:*

**Table 2: Statistical performance of the Random Forest algorithm in the spatial prediction of geomorphic indices (50 predictions).**

| Variable | $R^2$ | CV (%) $R^2$ | RMSE | CV (%) RMSE | MAE | CV % MAE |
|---|---|---|---|---|---|---|
| | Training | | | | | |
| SLt | 0.14 (± 0.02) | 15.57 | 9.21 (± 0.23) | 2.46 | 6.64 (± 0.15) | 2.28 |
| SLs | 0.23 (± 0.02) | 10.59 | 104.84 (± 5.26) | 5.02 | 68.10 (± 2.16) | 3.18 |
| SLs/SLt | 0.15 (± 0.02) | 13.92 | 4.53 (± 0.14) | 3.11 | 3.24 (± 0.08) | 2.54 |
| $K_{sn}$ | 0.39 (± 0.02) | 5.74 | 25.39 (± 1.27) | 5.01 | 17.42 (± 0.56) | 3.22 |
| | Validation | | | | | |
| SLt | 0.14 (± 0.03) | 24.79 | 9.30 (± 0.51) | 5.53 | 6.61(± 0.51) | 4.19 |
| SLs | 0.22 (± 0.04) | 18.10 | 104.11 (± 12.45) | 11.95 | 67.60 (± 12.45) | 4.97 |
| SLs/SLt | 0.13 (± 0.04) | 28.11 | 4.51 (± 0.32) | 7.10 | 3.20 (± 0.32) | 4.62 |
| $K_{sn}$ | 0.37 (± 0.05) | 13.82 | 26.15 (± 2.95) | 11.26 | 17.61 (± 2.95) | 5.72 |

In the spatial distribution of the indices (Figure 5), the highest SLt, SLs, SLs/SLt, and $k_{sn}$ values are mainly on plateaus and steep zones of the basin, where lithologies of the Areado and Mata da Corda Group occur. The indices tend to rise in the areas of geological faults, for example, in downstream of the basin, a fact more evident in the SLt and $k_{sn}$ indices.

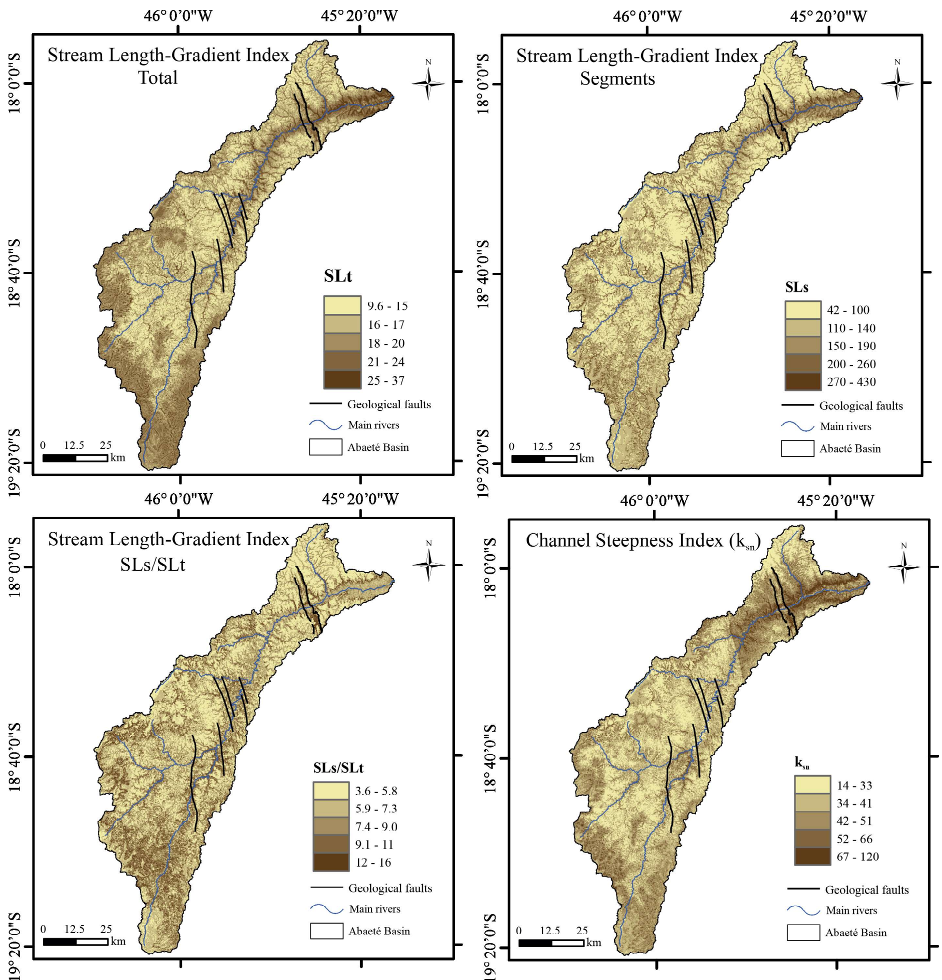


*Figure 5 - verage maps of geomorphic indices (SLt, SLs, SLs/SLt, and ksn) from the Random Forest algorithm.*

The distribution of indices (SLt, SLs, SLs/SLt, $k_{sn}$) by geological units (Figure 6), showed the highest averages in rocks of the Três Marias Formation in the downstream portion. In the sequence, the rocks of the Serra de Santa Helena Formation showed high averages, and this lithology occupies a small territorial extension and has only 18 points (knickpoints). In the Mata da Corda Group with 41 knickpoints, the average of the SLt was similar concerning other geological units. Moreover, in all indices there was a low variation trend, concentrating the values from the first to the third quartile and close to the average.

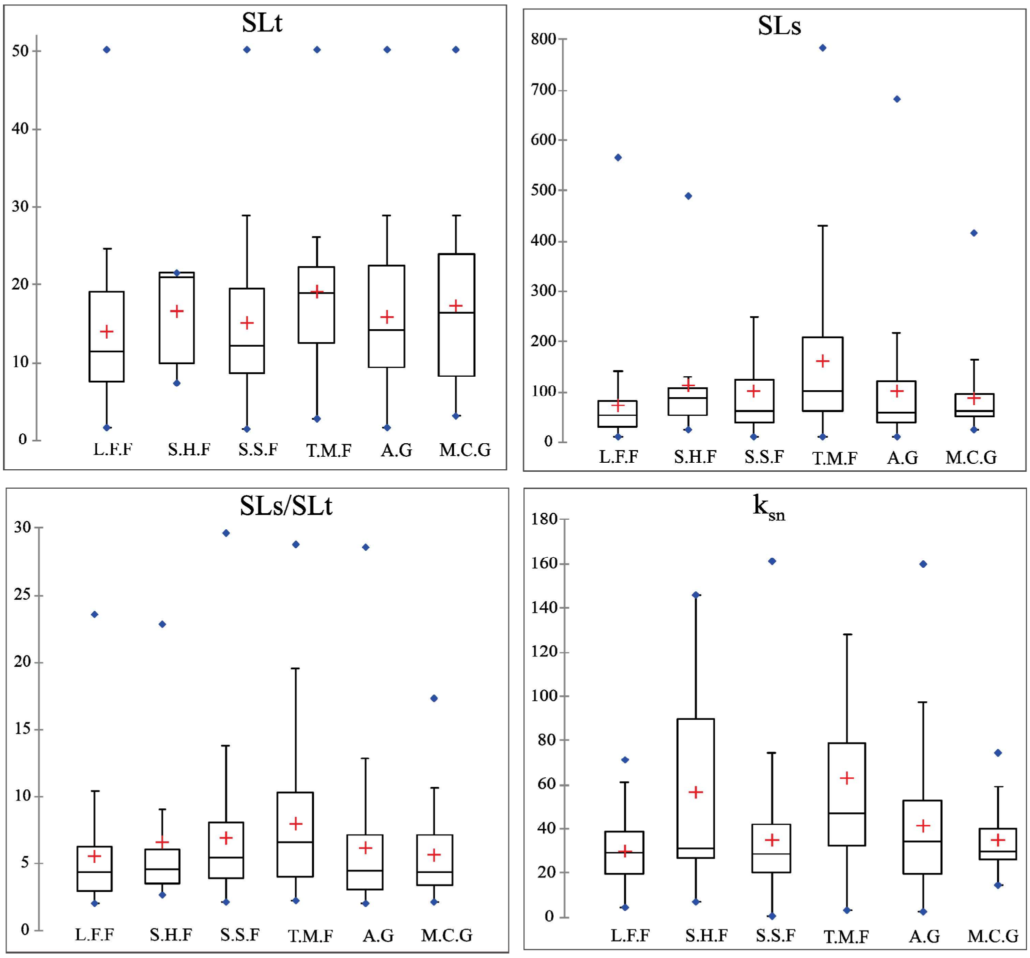


*Figure 6 - Mean, median, standard deviation, 1st and 3rd Quartile, near and far outliers and interquartile range of geomorphic indices (Stream Length – gradient index by total drainage extension (SLt), by segments (SLs), ratio (SLs / SLt); and Normalized Channel Steepness index (Ksn)). They are separated by geological domains: A.G: Areado Group; M.C.G: Mata da Corda Group; L.F.F: Lagoa Formosa Formation; T.M.F: Três Marias Formation; S.S F: Serra da Saudade Formation; S.S.H.F: Serra de Santa Helena Formation.*

## 4. Discussion

### 4.1 Prediction of geomorphic indices (SL e $k_{sn}$)

In spatial prediction, ML efficiency depends on three steps: (i) the $R^2$ values of the training and validation process cannot differ significantly; (ii) the contribution of predictive covariates to explain the spatial distribution of variables; and (iii) of the statistical levels of error of the prediction (YESILNACAR & TOPAL, 2005; KUHN & JOHNSON, 2013; SOUZA *et al.*, 2018; GOMES *et al.*, 2019).

The prediction of the indices indicated the best performance in $k_{sn}$ ($R^2$ 0.38) and the lowest in SLt ($R^2$ 0.25) (Table 1). Although there are no studies on the prediction of geomorphic indices by ML, there are studies in other areas that classify $R^2 < 0.50$ as good. for example, Gomes *et al.* (2019) studying carbon in the soil, identified $R^2$ from 0.28 to 0.32; and Yesilnacar & Topal (2005) in mapping landslides, obtained $R^2$ between 0.36 to 0.49. In general, the better performance of $R^2$ is highly dependent on the nature of a data set, as well as covariates that assist in the prediction.

A better indicator of ML performance is when the $R^2$ values of training and validation do not differ significantly (low overfitting) (KUHN & JOHNSON, 2013). Therefore, $R^2$ high in training and low in the validation process, indicates that the model is good at predicting with a portion of samples, but fails to predict in unsampled areas when subjected to validation, this being the main function of the model (MEYER *et al.*, 2018). Thus, in our results there was no overfitting and the model trains and validates appropriately (Table 2), and the architecture of the RF model contributes to low overfitting (BREIMAN, 2001). Furthermore, during the 50 predictions the values of $R^2$ varied little (CV%).

Regarding the selection of predictive covariates, three covariates were predominant (Table 1). The Ls-factor, as it measures the length and gradient of the slope; Standardized Height, indicates the vertical distance between the base and standardized slope index; e Morphometric Protection Index, a measure of the openness/protection calculated by analyzing the degree to which the surrounding relief protects the given cell. In all cases, the predominance of these covariates is consistent, since the indices (SL and $k_{sn}$) are related to changes in slope, being a predominant aspect in the covariates.

Concerning the uncertainty of prediction (Table 2), three characteristics of the error indicate good performance: (i) RMSE levels were below the average of the values of the indices (ii) RMSE e MAE during the 50 predictions varied little (CV%); and (iii) error levels were similar in training and validation. Therefore, statically the performance of RF in the prediction of geomorphic indices was satisfactory, and our results confirm that RF is a robust prediction algorithm, corroborating with other studies (NAWAR & MOUAZEN, 2017; GOMES *et al.*, 2019).

**4.2 Spatial variability of geomorphic indices and longitudinal profile**

The region of steep terrain in the south of the basin, where there are rocks from the Mata da Corda and Areado Groups, predominates sub-basins tilted to the right (AF = 61 to 73) (Figure 3 and Figure 1). The concentration and predominance of the same tilting direction are indicative of a common structural control among the sub-basins. In general, we observed that there are geological faults that tend to be perpendicular to the main river of the sub-basins. However, when tipping is by neotectonics, the geological faults are located close to the central axis of the basin (SALAMUNI *et al.*, 2008), and only in sub-basins 1 and 4 did it show this characteristic.

The lithology can promote a structural control generating asymmetric basin (EL HAMDOUNI *et al.*, 2008). Therefore, some characteristics of the Mata da Corda Group can control the landforms, forming plateaus (OLIVEIRA & RODRIGUES, 2007). The presence of ferruginous laterites and compact lithologies (Figure 7A and Figure 7B) inhibits vertical and lateral water flow (BAGGIO *et al.*, 2015). However, the underlying rocks (Areado Group) do not have the same lithological resistance, and this favors the formation of cliffs on the plateaus and altitude gradient influences the configuration of the sub-basins.

The reactivation of geological faults is not the main factor for tilting sub-basins in the region. For example, in sub-basin 4 (AF = 73), there is a geological fault parallel to the main river, coinciding with an escarpment, which even controls drainage, as the main river presents an inflection for SE (~ 90°) (Figure 3). However, the origin of the fault is related to the Graben/Horst system, originated during the South Atlantic rift phase (FRAGOSO *et al.*, 2011). In this sector, due to the distinct lithological resistance in the contact of the Mata Corda/Areado Groups, it favors the asymmetry of the basin.

The Mata da Corda Group protects the top of the relief, forming a residual plateau with escarpments with high sinuosity (OLIVEIRA & RODRIGUES, 2007) (Figure $3B_1$). The sinuosity is indicative of the non-reactivation of geological faults in the Quaternary, since in mountain fronts bounded by active faults tend to have a linear geometry (KELLER & PINTER, 1996; MODENESI-GAUTTIERI *et al.*, 2002). However, the geological fault favors the erosive processes, contributing to the formation of steep slopes, and this influences the asymmetric basins.

Although our analyzes do not indicate reactivation of geological faults, this does not extinguish the occurrence of neotectonic processes. In some sectors, there are rectilinear relief forms associated with geological faults (Figure $3B_2$); therefore, we just indicate that this is not a significant factor in generating asymmetric sub-basins.

In the plateaus and escarpments, the indices values are higher (SL, SLs, SLs/SLt and $k_{sn}$); we attribute this result to the elevation gradient in zones of lithological contact. This fact is evident when we observe the longitudinal profile of the rivers (Figure 4). In general, in the areas of contact between Cretaceous and Proterozoic, the profile assumes a steep slope (Cretaceous), and a smoother profile (Proterozoic). This behavior is because the sediments of the Areado Group have less resistance than the Proterozoic rocks (Figure 7C).

In general, steep river channels due to resistant rocks, has low incision rates of the channel, while channels steep due to rapid rock uplift rates, then both channel incision and hillslope erosion should be high (CYR *et al.*, 2014). Therefore, this last characteristic does not occur, a fact evident in sub-basins 5, 6, 7, and 8 (Figure 4).

The old landforms (Graben/Horst system) (FRAGOSO *et al.*, 2011), also influence the drainage and configuration of sub-basins. Over time, the ablation of part of the sediments that filled the Graben (FRAGOSO *et al.*, 2011; BAGGIO *et al.*, 2015) forming escarpments at the edges of the plateaus (OLIVEIRA & RODRIGUES, 2007), exposing rocks with different lithological resistances, favoring the formation of knickpoints. Therefore, these changes are reflected in the longitudinal profile. According to Larue (2008), the knickzones of lithological origin maintain strong vertical stability during all the river incision stages, and this characteristic occurs in sub-basins 4, 5 and 6 (Figure 4), however, in areas with less lithological variation along the river, the profile assumes a more stable configuration concerning the best fit line, for example, sub-basins 7 and 8 (Figure 4).

Another fact that influences drainage is the shear zones. The origin of the magmatism of the Mata da Corda Group is also related to shearing (CAMPOS & DARDENNE, 1997; FRAGOSO *et al.*, 2011). Therefore, in shear zones are areas of weakness and forms a sharp change in slope, as in the sub-basin 4 geological fault (Figure 3). Furthermore, the magmatism process also influenced the Bambuí Group because magmatism generated folding slopes and uplift of sedimentary strata (CAMPOS & DARDENNE, 1997). This factor can also confer higher resistance to rocks and forming knickpoints, including in the contact zones (Cretaceous/Proterozoic), the SL and $k_{sn}$ indexes remain high (Figure 1).

The SL and $k_{sn}$ indexes are also high downstream from the basin, presumably related to sets of geological faults (NW - SE), in the rocks of the Serra de Santa Helena Formation. Besides, the Bambuí Group rocks have distinct diagenetic stages (CAMPOS *et al.*, 2015)2015, influencing the incision capacity of the drainage. This characteristic is evident in some sections of the longitudinal profile of sub-basins 1, 2 and 3 (Figure 4), since in the Três Marias Formation, the longitudinal profile becomes convex or rectilinear; even the Metarenite and Siltstone typical of the unit are very silicified (Figure 7D) (CHAVES *et al.*, 2013).

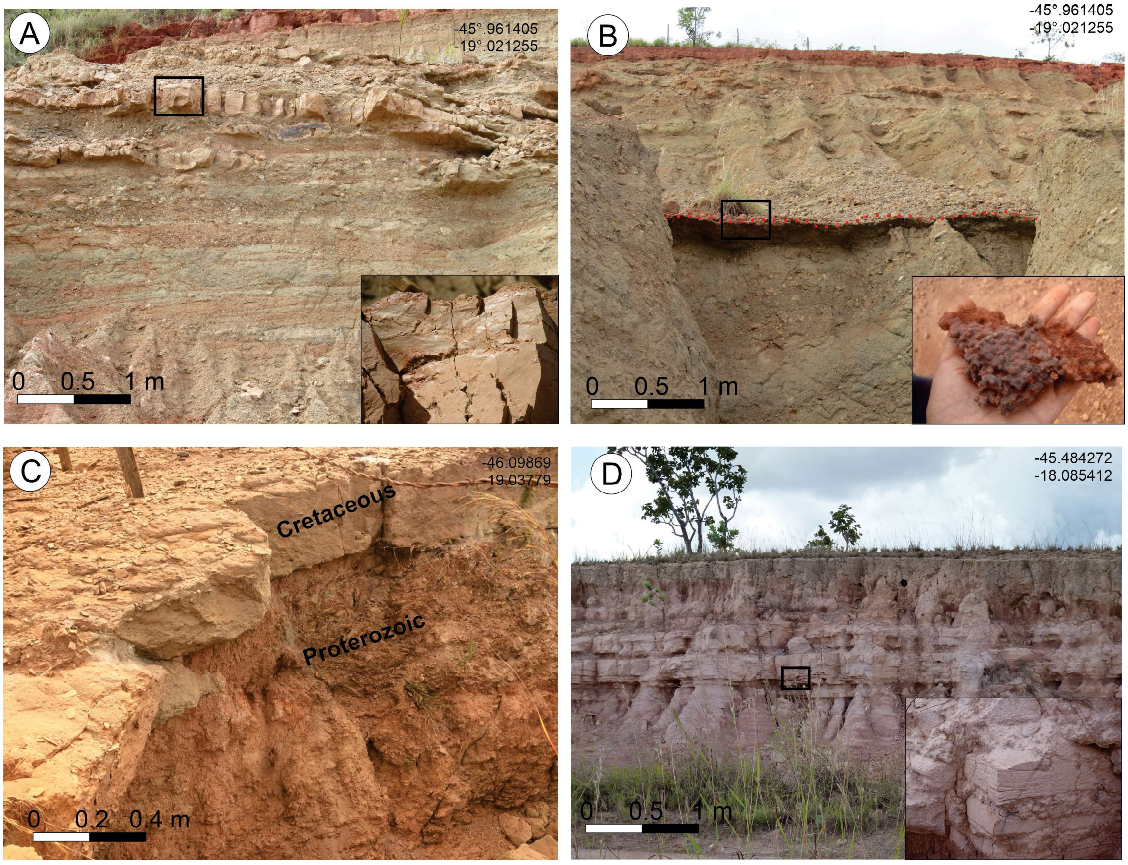


*Figure 7 - (A e B) Rocks of the Mata da Corda Group, with emphasis on resistant/compact lithology (A) and ferruginous concretion band (B); (C) Erosive discordance between Proterozoic sediments (Lagoa Formosa Formation) and Cretaceous sediments (Areado Group); (D) Metapelitic rocks of the Bambuí Group of the Três Marias Formation emphasizing the strata.*

In the Bambuí Group, studies indicate that there is a generalized fracturing that controls the current drainage morphology (IGLESIAS & UHLEIN, 2009), and this aspect reinforces that the lithological resistance influences higher values of the geomorphic indices. Therefore, in the basin, the high geomorphic indices, tilted basins and anomalies in the longitudinal profile, are more related to structural control by lithological resistance and reactivation of Proterozoic geological faults during the Cretaceous and derived implications. Our results do not exclude the possibility of neotectonics, including studies showing this effect in the Bambuí Group (CAMPOS & DARDENNE, 1997; CAMPOS et al., 2016). However, neotectonic is not an essential drainage control factor in the study area.

## Conclusions

In the basin, structural factors influence drainage strongly, and these factors are interconnected. There is a differential erosion due to zones of lithological contact, geological faults of the Proterozoic, and ancient configuration of the relief (Graben/Horst). These factors favored the formation of topographic unevenness, influencing the tilting of sub-basins.

The zones of lithological contact (Mata da Corda/Areado Groups and Proterozoic/Cretaceous rocks) contribute to the formation of knickpoints, with high values of geomorphic indices (SL and $k_{sn}$). The analysis of the longitudinal profile of the drainage confirms this information since areas of uplift or subsidence of the profile coincide with zones of lithological changes.

The Random Forest Algorithm (RF) can be used to predict geomorphic indices (SL and ksn). The similarity of $R^2$ values in the training and validation process demonstrates that the RF can predict in unsampled areas, creating maps with zones of influence (knickzones). Furthermore, the prediction error was low (RMSE e MAE).

The RF performed the prediction selecting between 7 and 11 covariates and ranking by importance levels. The geomorphometric covariates predominated. However, in predicting of better performance ($k_{sn}$ $R^2$ 0.38), there was the selection of the geology covariate, this indicates that when inserting covariables with a better relationship with the geomorphic indices, it should positively affect.

## Acknowledgment

We thank the anonymous reviewers for their careful reading and valuable comments, which helped to improve the manuscript. To CAPES (Coordenação de Aperfeiçoamento de Pessoal de Nível Superior), for granting a postdoctoral scholarship to the first and second authors. To the geoprocessing laboratory (Universidade Federal de Viçosa) for technical support.

## References

ALVES, F. C.; FÁTIMA ROSSETTI, D.; MORISSON VALERIANO, M.; OLIVEIRA ANDRADES FILHO, C. Neotectonics in the South American Passive Margin: Evidence of Late Quaternary Uplifting in the Northern Paraiba Basin (Ne Brazil). **Geomorphology**, v. 325, p. 1-16, 2019. DOI: 10.1016/j.geomorph.2018.09.028

AMBILI, V.; NARAYANA, A. C. Tectonic Effects on the Longitudinal Profiles of the Chaliyar River and Its Tributaries, Southwest India. **Geomorphology**, v. 217, p. 37-47, 2014. DOI: 10.1016/j.geomorph.2014.04.013

BAGGIO, H.; HORN, A. H.; TRINDADE, W.; RIBEIRO, E. O Grupo Mata da Corda na Bacia Hidrográfica do Rio do Formoso e suas Feições Morfológicas Correlatas. **Unimontes Científica**, v. 9, n. 1, p. 83-90, 2015.

BREIMAN, L. Random Forests. **Machine Learning**, v. 45, n. 1, p. 5-32, 2001. DOI: 10.1023/a:1010933404324

CAMPOS, J. E. G.; DARDENNE, M. A. Estratigrafia e Sedimentação da Bacia Sanfranciscana. **Revista Brasileira de Geociências**, v. 27, n. 3, p. 269-282, 1997.

CAMPOS, L. F. B.; GUIMARÃES, E. M.; BARROSO, R. H. G.; GOMES, A. W. Influência da Pressão e Temperatura na Cristalinidade da Illita em Sequências Proterozoicas: Norte do Distrito Federal e Goiás, Brasil. **Brazilian Journal of Geology**, v. 45, n. 3, p. 383, 2015. DOI: 10.1590/2317-488920150030268

CASTILLO, M.; MUÑOZ-SALINAS, E.; FERRARI, L. Response of a Landscape to Tectonics Using Channel Steepness Indices (Ksn) and Osl: A Case of Study from the Jalisco Block, Western Mexico. **Geomorphology**, v. 221, p. 204-214, 2014. DOI: 10.1016/j.geomorph.2014.06.017

CHAGAS, C. d. S.; JÚNIOR, W. d. C.; PINHEIRO, H. S. K.; XAVIER, P. A. M.; BHERING, S. B.; PEREIRA, N. R.; FILHO, B. C. Mapping Soil Cation Exchange Capacity in a Semiarid Region through Predictive Models and Covariates from Remote Sensing Data. **Revista Brasileira de Ciência do Solo**, v. 42,

2018. DOI: 10.1590/18069657rbcs20170183.

CHAVES, M. L. d. S. C.; BENITEZ, L.; ANDRADE, K. W.; QUEIROGA, G. N. Estratigrafia e Evolução Geomorfológica do Grupo Bambuí na Região de Morro da Garça (Mg). **Revista Geonomos**, v. 15, n. 2, 2013. DOI: 10.18285/geonomos.v15i2.97

CLODOALVES, J. Random Forest Techniques for Spatial Interpolation of Evapotranspiration Data from Brazilian's Northeast. **Computers and electronics in agriculture**, v. 166, p. 2019, 2019. DOI: 10.1016/j.compag.2019.105017

CRACKNELL, M. J.; READING, A. M.; MCNEILL, A. W. Mapping Geology and Volcanic-Hosted Massive Sulfide Alteration in the Hellyer–Mt Charter Region, Tasmania, Using Random Forests™ and Self-Organising Maps. **Australian Journal of Earth Sciences**, v. 61, n. 2, p. 287-304, 2014. DOI: 10.1080/08120099.2014.858081

CYR, A. J.; GRANGER, D. E.; OLIVETTI, V.; MOLIN, P. Distinguishing between Tectonic and Lithologic Controls on Bedrock Channel Longitudinal Profiles Using Cosmogenic 10be Erosion Rates and Channel Steepness Index. **Geomorphology**, v. 209, p. 27-38, 2014. DOI: 10.1016/j.geomorph.2013.12.010

DORANTI-TIRITAN, C.; HACKSPACHER, P. C.; SOUZA, D. H. d.; SIQUEIRA-RIBEIRO, M. C. The Use of the Stream Length-Gradient Index in Morphotectonic Analysis of Drainage Basins in Poços De Caldas Plateau, Se Brazil. **International Journal of Geosciences**, v. 5, n. 11, p. 12, 2014. DOI: 10.4236/ijg.2014.511112

EL HAMDOUNI, R.; IRIGARAY, C.; FERNÁNDEZ, T.; CHACÓN, J.; KELLER, E. A. Assessment of Relative Active Tectonics, Southwest Border of the Sierra Nevada (Southern Spain). **Geomorphology**, v. 96, n. 1–2, p. 150-173, 2008. DOI: http://dx.doi.org/10.1016/j.geomorph.2007.08.004

ETCHEBEHERE, M. L.; SAAD, A. R.; FULFARO, V. J.; PERINOTTO, J. A. d. J. Aplicação do Índice" Relação Declividade-Extensão-RDE" na Bacia do Rio do Peixe (SP) Para Detecção de Deformações neotectônicas. **Geologia USP. Série Científica**, v. 4, n. 2, p. 43-56, 2004. DOI: 10.5327/S1519-874X2004000200004

FODOR, R. V.; HANAN, B. B. Geochemical Evidence for the Trindade Hotspot Trace: Columbia Seamount Ankaramite. **Lithos**, v. 51, n. 4, p. 293-304, 2000. DOI: 10.1016/S0024-4937(00)00002-5

FONT, M.; AMORESE, D.; LAGARDE, J.-L. Dem and Gis Analysis of the Stream Gradient Index to Evaluate Effects of Tectonics: The Normandy Intraplate Area (NW France). **Geomorphology**, v. 119, n. 3–4, p. 172-180, 2010. DOI: 10.1016/j.geomorph.2010.03.017

FRAGOSO, D. G. C.; UHLEIN, A.; SANGLARD, J. C. D.; SUCKAU, G. L.; GUERZONI, H. T. G.; FARIA, P. H. Geologia dos Grupos Bambuí, Areado e Mata da Corda na Folha Presidente Olegário (1: 100.000), MG: Registro Deposicional do Neoproterozóico ao Neocretáceo da Bacia do São Francisco. **Revista Geonomos**, v. 19, n. 1, 2011. DOI: 10.18285/geonomos.v19i1.60

GARROTE, J.; GARZÓN HEYDT, G.; COX, R. T. Multi-Stream Order Analyses in Basin Asymmetry: A Tool to Discriminate the Influence of Neotectonics in Fluvial Landscape Development (Madrid Basin, Central Spain). **Geomorphology**, v. 102, n. 1, p. 130-144, 2008. DOI: 10.1016/j.geomorph.2007.07.023

GOMES, L. C.; FARIA, R. M.; SOUZA, E.; VELOSO, G. V.; SCHAEFER, C. E. G. R.; FERNANDES FILHO, E. I. Modelling and Mapping Soil Organic Carbon Stocks in Brazil. **Geoderma**, v. 340, p. 337-350, 2019. DOI: 10.1016/j.geoderma.2019.01.007

GRANITTO, P. M.; FURLANELLO, C.; BIASIOLI, F.; GASPERI, F. Recursive Feature Elimination with Random Forest for Ptr-Ms Analysis of Agroindustrial Products. **Chemometrics and Intelligent Laboratory Systems**, v. 83, n. 2, p. 83-90, 2006. DOI: 10.1016/j.chemolab.2006.01.007

GROHMANN, C. H.; RICCOMINI, C.; ALVES, F. M. Srtm-Based Morphotectonic Analysis of the Poços De Caldas Alkaline Massif, Southeastern Brazil. **Computers & Geosciences**, v. 33, n. 1, p. 10-19, 2007. DOI: 10.1016/j.cageo.2006.05.002

HACK, J. T. Stream-Profile Analysis and Stream-Gradient Index. **Journal of Research of the US Geological Survey**, v. 1, n. 4, p. 421-429, 1973.

HARE, P. W.; GARDNER, T. Geomorphic Indicators of Vertical Neotectonism Along Converging Plate Margins, Nicoya Peninsula, Costa Rica. *In*: Tectonic Geomorphology, Proceedings of the 15th Annual Binghamton Geomorphology Symposium, 1985, Boston. **Anais...** Boston: Allen and Unwin. 1985. p. 123-134.

IGLESIAS, M.; UHLEIN, A. Estratigrafia do Grupo Bambuí e Coberturas Fanerozóicas no Vale do Rio São Francisco, Norte de Minas Gerais. **Revista Brasileira de Geociências**, v. 39, n. 2, p. 256-266, 2009. DOI: 10.25249/0375-7536.2009392256266

JARVIS, A.; REUTER, H. I.; NELSON, A.; GUEVARA, E. **Hole-Filled Srtm for the Globe Version 4**, Available from the Cgiar-Csi Srtm 90m Database. 2008. http://srtm.csi.cgiar.org/ Access date: 01 April 2020.

KALE, V. S.; SENGUPTA, S.; ACHYUTHAN, H.; JAISWAL,

M. K. Tectonic Controls Upon Kaveri River Drainage, Cratonic Peninsular India: Inferences from Longitudinal Profiles, Morphotectonic Indices, Hanging Valleys and Fluvial Records. **Geomorphology**, v. 227, p. 153-165, 2014. DOI: 10.1016/j.geomorph.2013.07.027

KELLER, E. A.; PINTER, N. **Active Tectonics Earthquakes, Uplift, and Landscape**. New Jersey: Prentice Hall Upper Seddle River, 1996. 359p.

KUHN, M.; JOHNSON, K. **Applied Predictive Modeling**. 26. New York: Springer, 2013. 600p.

LARUE, J.-P. Effects of Tectonics and Lithology on Long Profiles of 16 Rivers of the Southern Central Massif Border between the Aude and the Orb (France). **Geomorphology**, v. 93, n. 3, p. 343-367, 2008. DOI: 10.1016/j.geomorph.2007.03.003

LIMA, O. N. B.; UHLEIN, A.; BRITTO, W. Estratigrafia do Grupo Bambuí na Serra da Saudade e Geologia do Depósito Fosfático de Cedro do Abaeté, Minas Gerais. **Revista Brasileira de Geociências**, v. 37, n. 4 suppl, p. 204-215, 2007.

MEYER, H.; REUDENBACH, C.; HENGL, T.; KATURJI, M.; NAUSS, T. Improving Performance of Spatio-Temporal Machine Learning Models Using Forward Feature Selection and Target-Oriented Validation. **Environmental Modelling & Software**, v. 101, p. 1-9, 2018. DOI: 10.1016/j.envsoft.2017.12.001

MODENESI-GAUTTIERI, M. C.; TAKASHI HIRUMA, S.; RICCOMINI, C. Morphotectonics of a High Plateau on the Northwestern Flank of the Continental Rift of Southeastern Brazil. **Geomorphology**, v. 43, n. 3, p. 257-271, 2002. DOI: 10.1016/S0169-555X(01)00137-4

MOHAMMADY, M.; POURGHASEMI, H. R.; AMIRI, M. Land Subsidence Susceptibility Assessment Using Random Forest Machine Learning Algorithm. **Environmental Earth Sciences**, v. 78, n. 16, p. 503, 2019. DOI: 10.1007/s12665-019-8518-3

MONTEIRO, K. d. A.; MISSURA, R.; CORREA, A. C. d. B. Application of the Hack Index - or Stream Length-Gradient Index (Sl Index) - to the Tracunhaém River Watershed, Pernambuco, Brazil. **Geociências**, v. 29, p. 533-539, 2010.

NAWAR, S.; MOUAZEN, A. M. Comparison between Random Forests, Artificial Neural Networks and Gradient Boosted Machines Methods of on-Line Vis-Nir Spectroscopy Measurements of Soil Total Nitrogen and Total Carbon. **Sensors**, v. 17, n. 10, p. 1-22, 2017. DOI: 10.3390/s17102428

OLIVEIRA, P. C. A.; RODRIGUES, S. C. Cartografia Do Relevo: Um Estudo Aplicado Na Região Oeste De Minas Gerais. **Revista Brasileira de Geomorfologia**, v. 8, n. 2, p. 37-44, 2007. DOI: 10.20502/rbg.v8i2.91

OLIVER, M. A.; WEBSTER, R. Kriging: A Method of Interpolation for Geographical Information Systems. **International Journal of Geographical Information Systems**, v. 4, n. 3, p. 313-332, 1990. DOI: 10.1080/02693799008941549

PÉREZ-PEÑA, J.; AZAÑÓN, J.; AZOR, A.; DELGADO, J.; GONZÁLEZ-LODEIRO, F. Spatial Analysis of Stream Power Using Gis: Slk Anomaly Maps. **Earth Surface Processes and Landforms**, v. 34, n. 1, p. 16-25, 2009. DOI: 10.1002/esp.1684

PINTO, C.; SILVA, L.; LEITE, C. **Mapa Geológico Do Estado De Minas Gerais, 1: 1.000. 000.** CODEMIG, Belo Horizonte.

QUEIROZ, G. L.; SALAMUNI, E.; NASCIMENTO, E. R. Knickpoint Finder: A Software Tool That Improves Neotectonic Analysis. **Computers & Geosciences**, v. 76, p. 80-87, 2015. DOI: 10.1016/j.cageo.2014.11.004

RCORE, T. 2016. R: A Language and Environment for Statistical Computing. 26 Fevereiro 2020. Disponível em: http://www.R-project.org/. Access date: 01 April 2020.

SALAMUNI, E.; EBERT, H. D.; HASUI, Y. Morfotectônica Da Bacia Sedimentar De Curitiba. **Brazilian Journal of Geology**, v. 34, n. 4, p. 469-478, 2008. DOI: 10.25249/0375-7536.2004344469478

SANTOS, L. F. F. d.; GUEDES, I. C.; ETCHEBEHERE, M. L. Análise Neotectônica do Pontal do Paranapanema (SP) Mediante Aplicação de Parâmetros Fluviomorfométricos. **Geociências (São Paulo)**, v. 30, n. 4, p. 491-507, 2011.

SCHWANGHART, W.; SCHERLER, D. Short Communication: Topotoolbox 2 - Matlab-Based Software for Topographic Analysis and Modeling in Earth Surface Sciences. **Earth Surface Dynamics**, v. 2, n. 1, p. 1-7, 2014. DOI: 10.5194/esurf-2-1-2014

SEEBER, L.; GORNITZ, V. River Profiles Along the Himalayan Arc as Indicators of Active Tectonics. **Tectonophysics**, v. 92, n. 4, p. 335-367, 1983. DOI: 10.1016/0040-1951(83)90201-9

SENA, N. C.; VELOSO, G. V.; FILHO, E. I. F.; FRANCELINO, M. R.; SCHAEFER, C. E. G. R. Analysis of Terrain Attributes in Different Spatial Resolutions for Digital Soil Mapping Application in Southeastern Brazil. **Geoderma Regional**, p. e00268, 2020. DOI: 10.1016/j.geodrs.2020.e00268

SGARBI, G. N. C. The Cretaceous Sanfranciscan Basin, Eastern Plateau of Brazil. **Revista Brasileira de Geociências**, v. 30, n. 3, p. 450-452, 2000. DOI: 10.25249/0375-7536.2000303450452

SOUZA, A. O.; PEREZ FILHO, A. Aplicação Do Ksn Index E

Do Sl Index No Estudo Dos Knickpoints No Perfil Longitudinal Do Rio Ribeira De Iguape-Sp. **Revista do Departamento de Geografia**, v. special, p. 208-217, 2017. DOI: 10.11606/rdg.v0ispe.132180

SOUZA, C. M. P.; THOMAZINI, A.; SCHAEFER, C. E. G. R.; VELOSO, G. V.; MOREIRA, G. M.; FERNANDES FILHO, E. I. Multivariate Analysis and Machine Learning in Properties of Ultisols (Argissolos) of Brazilian Amazon. **Revista Brasileira de Ciência do Solo**, v. 42, p. 1 - 20, 2018. DOI: 10.1590/18069657rbcs20170419

SOUZA, D. V.; MARTINS, A. A.; FARIA, A. L. L. Aplicação do Índice de Hack (SL) a um Trecho do Rio Zêzere, Portugal. **Revista Brasileira de Geomorfologia**, v. 12, n. 1, 2011. DOI: 10.20502/rbg.v12i1.215

STRAHLER, A. N. Quantitative Analysis of Watershed Geomorphology. **Eos, Transactions American Geophysical Union**, v. 38, n. 6, p. 913-920, 1957. DOI: 10.1029/TR038i006p00913

TROIANI, F.; GALVE, J. P.; PIACENTINI, D.; DELLA SETA, M.; GUERRERO, J. Spatial Analysis of Stream Length-Gradient (Sl) Index for Detecting Hillslope Processes: A Case of the Gállego River Headwaters (Central Pyrenees, Spain). **Geomorphology**, v. 214, p. 183-197, 2014. DOI: 10.1016/j.geomorph.2014.02.004

UHLEIN, G. J.; UHLEIN, A.; PEREIRA, E.; CAXITO, F. A.; OKUBO, J.; WARREN, L. V.; SIAL, A. N. Ediacaran Paleoenvironmental Changes Recorded in the Mixed Carbonate-Siliciclastic Bambuí Basin, Brazil. **Palaeogeography, Palaeoclimatology, Palaeoecology**, v. 517, p. 39-51, 2019. DOI: 10.1016/j.palaeo.2018.12.022

WOBUS, C.; WHIPPLE, K. X.; KIRBY, E.; SNYDER, N.; JOHNSON, J.; SPYROPOLOU, K.; CROSBY, B.; SHEEHAN, D.; WILLETT, S. Tectonics from Topography: Procedures, Promise, and Pitfalls. **Special papers-geological society of america**, v. 398, p. 55, 2006. DOI: 10.1130/2006.2398(04)

YESILNACAR, E.; TOPAL, T. Landslide Susceptibility Mapping: A Comparison of Logistic Regression and Neural Networks Methods in a Medium Scale Study, Hendek Region (Turkey). **Engineering Geology**, v. 79, n. 3, p. 251-266, 2005. DOI: 10.1016/j.enggeo.2005.02.002